A multi-beam X-ray imaging detector using a branched optical fiber bundle

著者	Wataru Yashiro, Tetsuroh Shirasawa, Chika Kamezawa, Wolfgang Voegeli, Etsuo Arakawa, Kentaro Kajiwara
journal or publication title	Japanese Journal of Applied Physics
volume	59
number	3
page range	038003
year	2020-03-06
URL	http://hdl.handle.net/10097/00131039

doi: 10.35848/1347-4065/ab79fd

A multi-beam X-ray imaging detector using a branched optical fiber bundle

Wataru Yashiro[1]*, Tetsuroh Shirasawa[2], Chika Kamezawa[1,3,4], Wolfgang Voegeli[5], Etsuo Arakawa[5], and Kentaro Kajiwara[6]

[1] *Institute of Multidisciplinary Research for Advanced Materials (IMRAM), Tohoku University, Sendai, Miyagi 980-5780, Japan*

[2] *National metrology institute of Japan (NMIJ), National Institute of Advanced Industrial Science and Technology (AIST), Tohoku University, Sendai, Miyagi 980-5780, Japan*

[3] *Department of Materials Structure Science, SOKENDAI (The Graduate University for Advanced Studies), 1-1 Oho, Tsukuba, Ibaraki 305-0801, Japan*

[4] *Institute of Materials Structure Science/ KEK, 1-1 Oho, Tsukuba, Ibaraki 305-0801, Japan*

[5] *Faculty of Education, Tokyo Gakugei University, Koganei, Tokyo 184-8501, Japan*

[6] *Japan Synchrotron Radiation Research Institute (JASRI), Tsukuba, Ibaraki 305-8560, Japan*

We developed a multi-beam X-ray imaging detector, consisting of four scintillator screens connected by a branched optical fiber bundle with a CMOS camera. By using the detector and a multi-beam imaging optics with silicon single crystalline blades designed for a white synchrotron radiation source, we successfully demonstrated multi-beam X-ray imaging with an exposure time of 1 ms. The long and flexible optical fiber bundle used for the detector enables us to realize high-speed multi-beam X-ray imaging with high flexibility at a low cost.

X-ray imaging is a powerful tool for two- and three-dimensional visualization of inner structures in samples that are opaque to visible light. A two-dimensional projection image is easily obtained with a simple experimental setup consisting of an X-ray source and an X-ray imaging detector. Synchrotron radiation (SR) sources and X-ray free-electron laser (XFEL) have enabled us to realize even lower than μs temporal resolutions[1–10] with the help of X-ray phase-contrast imaging techniques such as the propagation-based imaging (PBI)[11–13] or grating-based imaging (GBI) techniques.[4,5,14–34] However, inner structures in the depth direction cannot be differentiated from the projection image. On the other hand, X-ray tomography allows us to visualize three-dimensional structures in a sample, but it typically requires hundreds of projection images, which are obtained by the rotation of the sample or of both the X-ray source and detector. Recently, X-ray tomography for rotating samples with

*E-mail: wyashiro@tohoku.ac.jp

a measurement time of a few ms and a spatial resolution of a few tens of μm was successfully realized by using a white SR source.[4,5,10,31] However, high-speed rotation of a sample with a few tens of thousands rpm hinders to precisely control the environment around the sample. In addition, the high-speed rotation cannot be applied to liquids and living animals because of the centrifugal force arising from the rotation.

Recently, a few X-ray multi-beam techniques have been proposed for SR sources and/or x-ray free-electron laser,[35–37] which can differentiate inner structures in the depth direction, and real-time multi-beam X-ray imaging with a temporal resolution less than 10 ms could be realized if the images projected by the multi-beams are simultaneously obtained. In this paper, we report on a multi-beam X-ray imaging detector, consisting of four scintillator screens connected by a branched optical fiber bundle with a CMOS camera. Using the detector, we successfully obtained five projection images with a temporal resolution of 1 ms.

Photos of the branched optical fiber bundle used for the multi-beam X-ray detector are shown in Fig. 1. Each optical fiber constituting the bundle has a diameter of 50 μm and a length of 2 m (SOG-70S 50 μm, SUMITA OPTICAL GLASS, Inc.), and can be flexibly bent. The bundle has four branches, each of which has three segments with a size of 5 mm $\times$ 7.5 mm (totally, 5 mm $\times$ 22.5 mm) and transmits images from one side to the other, as shown in the right figure of Fig. 1. The multi-beam X-ray detector was constructed by the branched optical fiber bundle, scintillator screens, relay lenses, and a CMOS camera for visible light (see Fig. 2). On the top of each branch of the bundle, the surface of a scintillator screen was fixed with optical oil sandwiched between them, and the other side was coupled with the relay lenses to the CMOS camera.

The experimental setup for multi-beam X-ray imaging using the detector is shown in Fig. 2. The experiment was performed at BL28B2 in SPring-8, Japan, where a white SR beam from a bending magnet is available. We employed a multi-beam X-ray optics consisting of four Si(001) single-crystalline blades with different angles to the impinging white SR beam,[37] each of which reflects X-rays satisfying the Bragg condition. We used the Laue-case reflections from the (110) crystal planes, which were designed to cross on the sample. The four reflected X-ray beams passed through a sample, and projected its images on scintillator screens (Mitsubishi Chemical Corporation, DRZ-HR (Gd_2O_2S: Tb, 50 μm)). The projected images on the screens were transmitted by the optical fiber bundle to its other side, and captured by a CMOS camera (Photron FASTCAM Mini AX50) with a pixel size of 20 μm $\times$ 20 μm through relay lenses with a magnification of 1. The white SR beam was also directly used for obtaining a projection image, which was captured by a high-spatial-resolution X-ray image detector (the inset of Fig. 2) with an effective pixel size of 4.6 μm consisting of a scintillator screen (Gd_2O_2S: Tb, 10 μm)), a mirror, relay lenses, and a CMOS camera (Photron FASTCAM Mini AX100).

For a demonstration of the multi-beam X-ray imaging, a USB flash memory was used as a sample. Figure 3 (a) shows a photo of the irradiated side of the sample. Figure 3 (b) shows a projection image (natural logarithm of the X-ray transmittance) of the sample with a large field of view, preliminarily obtained using a laboratory X-ray generator (RIGAKU Ultrax18 with a tungsten target, tube voltage 50 kV, tube current 10 mA, effective source size 0.1 mm (horizontal) $\times$ 0.2 mm (vertical)). The field of view corresponds to the area in the square shown in Fig. 3 (a). An X-ray imaging detector with an effective pixel size of 5.5 μm $\times$ 5.5 μm (Hamamatsu Photonics C14120-20P) based on a scintillator screen (50 μmu-thick $Lu_3Al_5O_{12}$: Ce), a fiber optic plate, and a CMOS camera was used with an exposure time of 1 s. Figures 3 (c1)-(c4) are the projection images corresponding to the area of the dotted square in Fig. 3 (b) obtained by the multi-beam imaging setup shown in Fig. 2. The four images were simultaneously obtained with an exposure time of 1 ms. Here, Figs. 3 (c1)-(c4) corresponds to beam 1, 2, 3, and 4 in Fig. 2, and the projection angles for the beams were 11.5°, 7.96°, -7.96°, and -14.9 °, corresponding to 32.1 keV, 46.5 keV, 46.5 keV, and 24.9 keV for the 220 Bragg reflection, respectively. It can be seen that the positions of electrode B and hole C shift relative to component A. This shift in the positions reflects the difference in the depths of A, B, and C. The spatial resolution of the images was 200 μm, which should be mainly determined by the thickness of the scintillator screen (50 μm), the diameter of the optical fiber (50 μm), and a finite distance between the scintillator screen and the surface of the optical fiber bundle. Figure 3 (d) is the projection image corresponding to the area of the dashed square in Fig. 3 (c2) obtained by using the white SR beam and the high-spatial-resolution X-ray imaging detector. The image was obtained with an exposure time of 0.1 ms and the spatial resolution of the image was 10 μm, although its field of view is smaller than those obtained by the multi-beam detector. Thus, we demonstrated that the setup simultaneously provides four projection images with an exposure time of 1 ms and a high-spatial resolution projection image with an exposure time of 0.1 ms.

From the shift of electrode B and hole C relative to component A, we can estimate the depth of B and C relative to A. From linear least-squares fittings to the shifts obtained from the four images of Fig. 3 (c1)-(c4), the depths of B and C were estimated to be -1.20 mm and -0.63 mm, respectively, where the positive direction of depth was taken in the direction of the impinging X-ray beam from upstream to downstream.

Fig. 1. Photos of optical fiber bundle used for multi-beam X-ray detector (left) and transmitted image on one side (right).

Fig. 2. Schematic illustration of experimental setup for multi-beam X-ray imaging using white synchrotron radiation (SR) beam at BL28B2 in SPring-8, Japan (top view). Inset: side view of high-spatial-resolution X-ray imaging detector for white SR beam.

Fig. 3. (a) Photo of irradiated (upstream) side of sample (USB flash memory). (b)-(d) Projection images (natural logarithm of X-ray transmittance) of sample. (b) Preliminarily obtained projection image of sample by using laboratory X-ray source with field of view shown in (a) (gray scale: −4.5-0.3). (c1)-(c4) Projection images obtained by multi-beam X-ray imaging detector for beam 1, 2, 3, and 4 in Fig. 2 (gray scale: −2.7-0.3). (d) Projection image obtained by directly using white synchrotron beam (gray scale: −4.5-0.3)

One of the advantages of the multi-beam X-ray imaging detector is its flexibility. The scintillator screens on the top of the branched optical fiber bundle can be flexibly allocated for various multi-beam X-ray imaging experiments including those for laboratory X-ray sources.[38–41] They can be located even inside a sample. In addition, the system can be realized at a lower cost than that required for several CMOS cameras. For these reasons, the multi-beam X-ray imaging detector reported in this paper should provide a promising approach for multi-beam X-ray imaging with a high speed and/or a high throughput.

In summary, we developed a four-beam X-ray imaging detector, consisting of four scintillator screens connected by a branched optical fiber bundle with a CMOS camera. By using the detector and a multi-beam imaging optics with silicon single crystalline blades designed for a white SR source, we successfully demonstrated five-beam X-ray imaging with an exposure time of 1 ms. The long and flexible optical fiber bundle used for the detector enables us to realize high-speed multi-beam X-ray imaging with high flexibility at a low cost.

Acknowledgments The experiment was performed in SPring-8, Japan. This research was supported by JST CREST Grant Number JPMJCR1765.

References

1) J.J. Socha, M.W. Westneat, J.F. Harrison, J.S. Waters, and W.K. Lee, BMC Biol. **5**, 6 (2007)
2) J.S. Lee, B.M. Weon, S.J. Park, J.H. Je, K. Fezzaa, and W.K. Lee, Nature Commun. **2**, 367 (2011).
3) A. Rack, M. Scheel, L. Hardy, C. Curfs, A. Bonnin, H. Reichert, J. Synchrotron Rad. **21**, 815 (2014).
4) W. Yashiro, D. Noda, and K. Kajiwara, Appl. Phys. Express **10**, 052501 (2017).
5) W. Yashiro, R. Ueda, K. Kajiwara, D. Noda, and H. Kudo, Jpn. J. Appl. Phys. **56**, 112503 (2017).
6) M. P. Olbinado, X. Just, J.-L. Gelet, P. Lhuissier, M. Scheel, P. Vagovic, T. Sato, R. Graceffa, J. Schulz, A. Mancuso, J. Morse, and A. Rack, Opt. Express **25**, 13857 (2017).
7) M. P. Olbinado, J. Grenzer, P. Pradel, T. De Resseguier, P. Vagovic, M.-C. Zdora, V.A. Guzenko, C. David, and A. Rack, J. Instrum. **13**, C04004 (2018).
8) E. M. Escauriza, M. P. Olbinado, M. E. Rutherford, D. J. Chapman, J. C. Z. Jonsson, A. Rack, and D. E. Eakins, Appl. Opt. **57**, 5004 (2018).
9) P. Vagovič, T. Sato, L. Mikeš, G. Mills, R. Graceffa, F. Mattsson, P. Villaueva-Perez, A. Ershov, T. Faragó, J. Uličný, H. Kirkwood, R. Letrun, R. Mokso, M.-C. Zdora, M. P. Olbinado, A. Rack, T. Baumbach, J. Schulz, A. Meents, H. N. Chapman, and A. P. Mancuso, Optica **6**, 1106 (2019).
10) F. García-Moreno, P.H. Kamm, T.R. Neu, F. Bülk, R. Mokso, C. M. Schlepütz, M. Stampanoni, and J. Banhart, Nat Commun. **10**, 3762 (2019).
11) A. Snigirev, I. Snigireva, V. Kohn, S. Kuznetsov, and I. Schelokov, Rev. Sci. Instrum. **66**, 5486 (1995).
12) S.W. Wilkins, T.E. Gureyev, D. Gao, A. Pogany, A.W. Stevenson, Nature **384**, 335 (1996).
13) P. Cloetens, R. Barrett, J. Baruchel, J.-P guigay, and M. Schlenker, J. Phys. D **29**, 133 (1996).
14) C. David, B. Nöhammer, and H. H. Solak, Appl. Phys. Lett. **81**, 3287 (2002).
15) A. Momose, S. Kawamoto, I. Koyama, Y. Hamaishi, K. Takai, and Y. Suzuki, Jpn. J. Appl. Phys. **42**, L866 (2003).
16) T. Weitkamp, A. Diaz, C. David, F. Pfeiffer, M. Stampanoni, P. Cloetens, and E. Ziegler, Opt. Express **13**, 6296 (2005).

17) A. Momose, W. Yashiro, and Y. Takeda, Jpn. J. Appl. Phys. **45**, 5254 (2006).
18) F. Pfeiffer, T. Weitkamp, O. Bunk, and C. David, Nat. Phys. **2**, 258 (2006).
19) W. Yashiro, Y. Takeda, and A. Momose, J. Opt. Soc. Am. A **25**, 2025 (2008).
20) A. Momose, W. Yashiro, and Y. Takeda, Jpn. J. Appl. Phys. **47**, 8077 (2008).
21) F. Pfeiffer, T. Weitkamp, O. Bunk, and C. David, Nat Mater. **7**, 134 (2008).
22) W. Yashiro, Y. Takeda, A. Takeuchi, Y. Suzuki, and A. Momose, Phys. Rev. Lett. **103**, 180801 (2009).
23) A. Momose, W. Yashiro, H. Maikusa, and Y. Takeda, Opt. Express **17**, 12540 (2009).
24) W. Yashiro, Y. Terui, K. Kawabata, and A. Momose, Opt. Express **18**, 16890 (2010).
25) W. Yashiro, S. Harasse, A. Takeuchi, Y. Suzuki, and A. Momose, Phys. Rev. A **82**, 043822 (2010).
26) H. Kuwabara, W. Yashiro, S. Harasse, H. Mizutani, and A. Momose, Appl. Phys. Express **4**, 062502 (2011).
27) A. Momose, H. Kuwabara, and W. Yashiro, Appl. Phys. Express **4**, 066603 (2011).
28) W. Yashiro, S. Harasse, K. Kawabata, H. Kuwabara, T. Yamazaki, and A. Momose, Phys. Rev. B **84**, 094106 (2011).
29) W. Yashiro and A. Momose, Opt. Express **23**, 9233 (2015).
30) W. Yashiro, P. Vagovič, and A. Momose, Opt. Express **23**, 23462 (2015).
31) W. Yashiro, C. Kamezawa, D. Noda, and K. Kajiwara, Appl. Phys. Express **11**, 122501 (2018).
32) W. Yashiro, D. Noda, and K. Kajiwara, Opt. Express **26**, 1012 (2018).
33) W. Yashiro, Microscopy **67**, 303 (2018).
34) W. Yashiro, S. Ikeda, Y. Wada, K. Totsu, Y. Suzuki, and A. Takeuchi, Sci. Rep. **9**, 14120 (2019).
35) M. Hoshino, T. Sera, K. Uesugi and N. Yagi, JINST **8**, C05002 (2013).
36) P. Villanueva-Perez, B. Pedrini, R. Mokso, P. Vagovic, V. A. Guzenko, S. J. Leake, P. R. Willmott, P. Oberta, C. David, H. N. Chapman, and M. Stampanoni, Optica **5**, 1521 (2018).
37) W. Voegeli, K. Kajiwara, H. Kudo, and W. Yashiro, to be published (2019).
38) M. Bieberle, F. Barthel, H.-J. Menz, H.-G. Mayer, and U. Hampel, Appl. Phys. Lett. **98**, 034101 (2011).
39) G. Yang, X.Qian, T.Phan, F.Sprenger, S.Sultana, X.Calderon-Colon, B.Kearse, D. Spronk, J.Lu, O.Zhou, Nucl. Instrum. Methods Phys. Res. A **648**, S220 (2011).
40) K. M. Sowa, B. R. Jany, and P. Korecki, Optica **5**, 577 (2018).

41) A. Cramer, J. Hecla, D. Wu, X. Lai, T. Boers, K. Yang, T. Moulton, S. Kenyon, Z. Arzoumanian, W. Krull, K. Gendreau and R. Gupta, Sci. Rep. **8**, 14195 (2018).

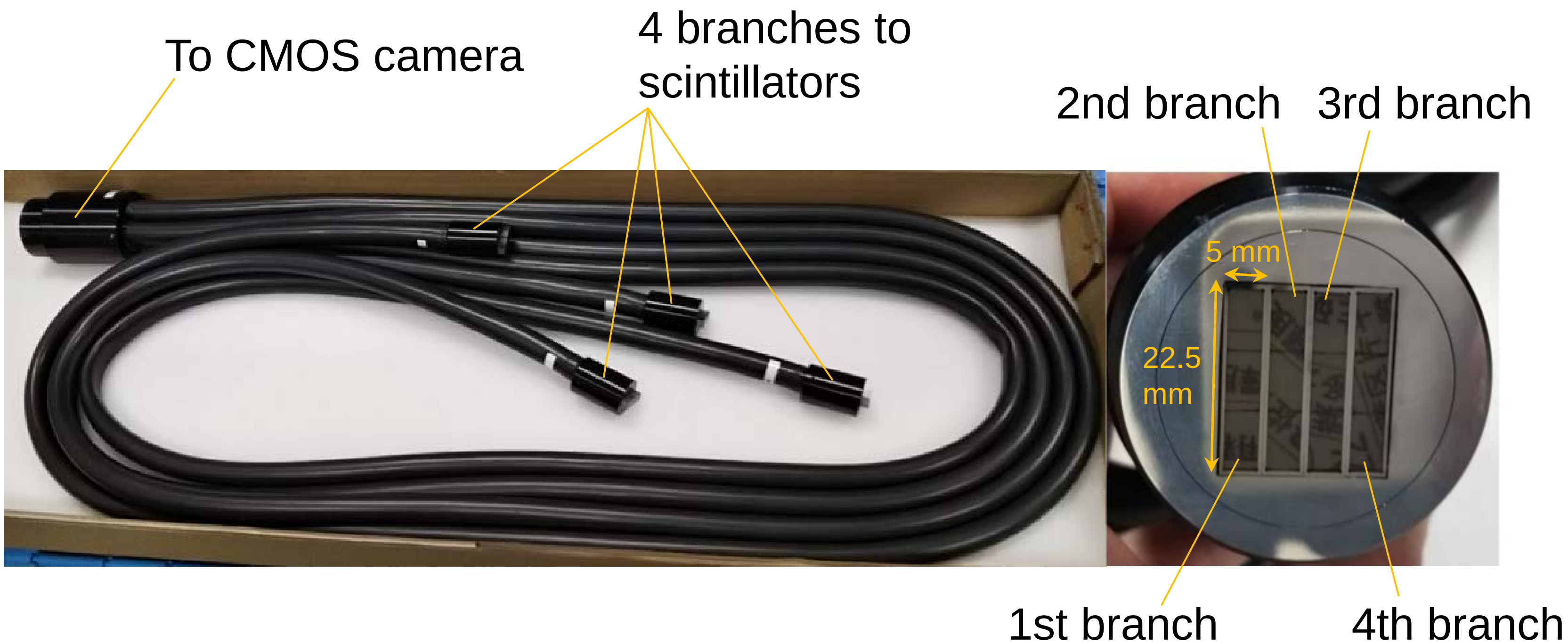

Fig. 1 W. Yashiro et al.

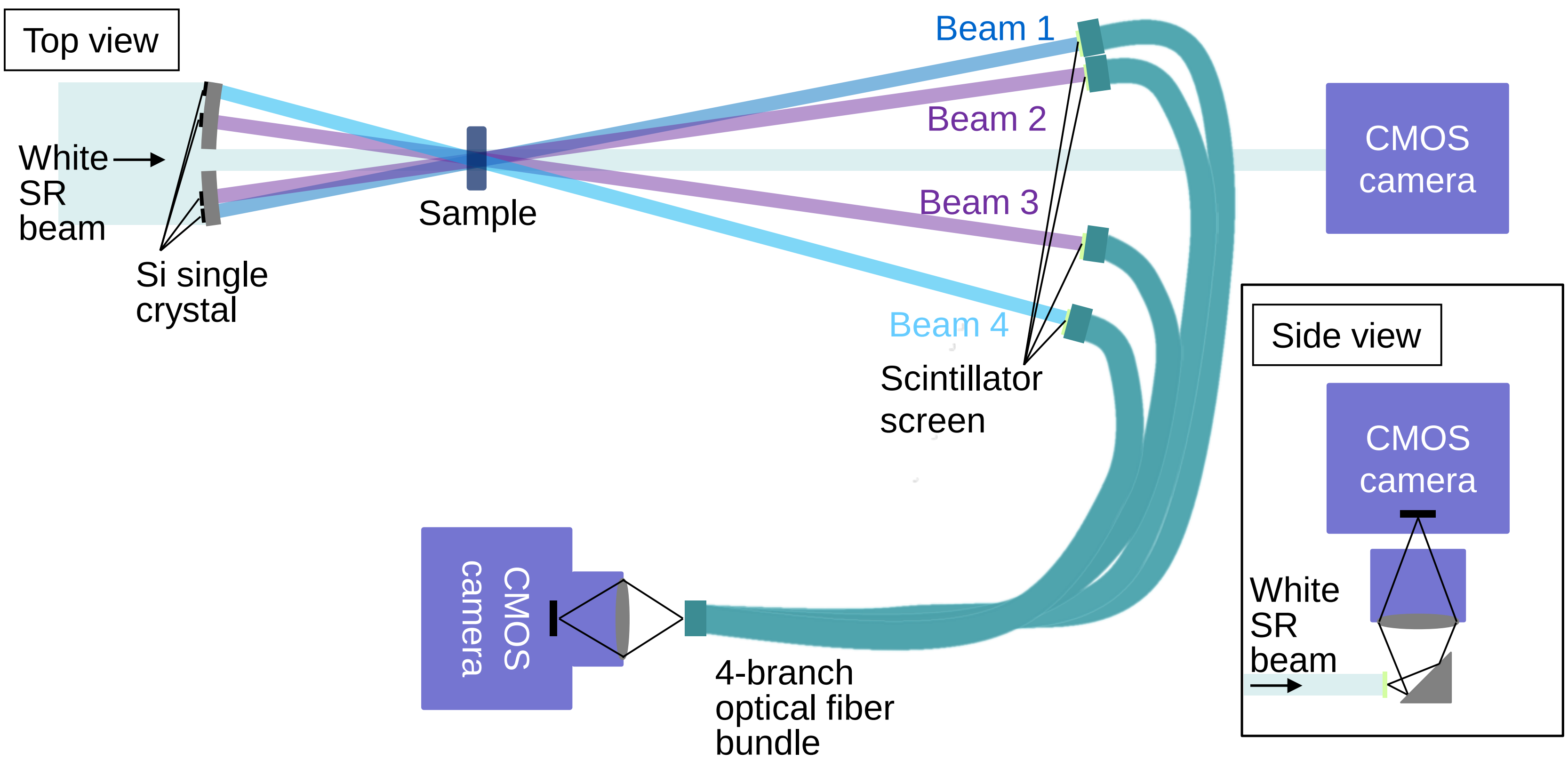

Fig. 2 W. Yashiro et al.

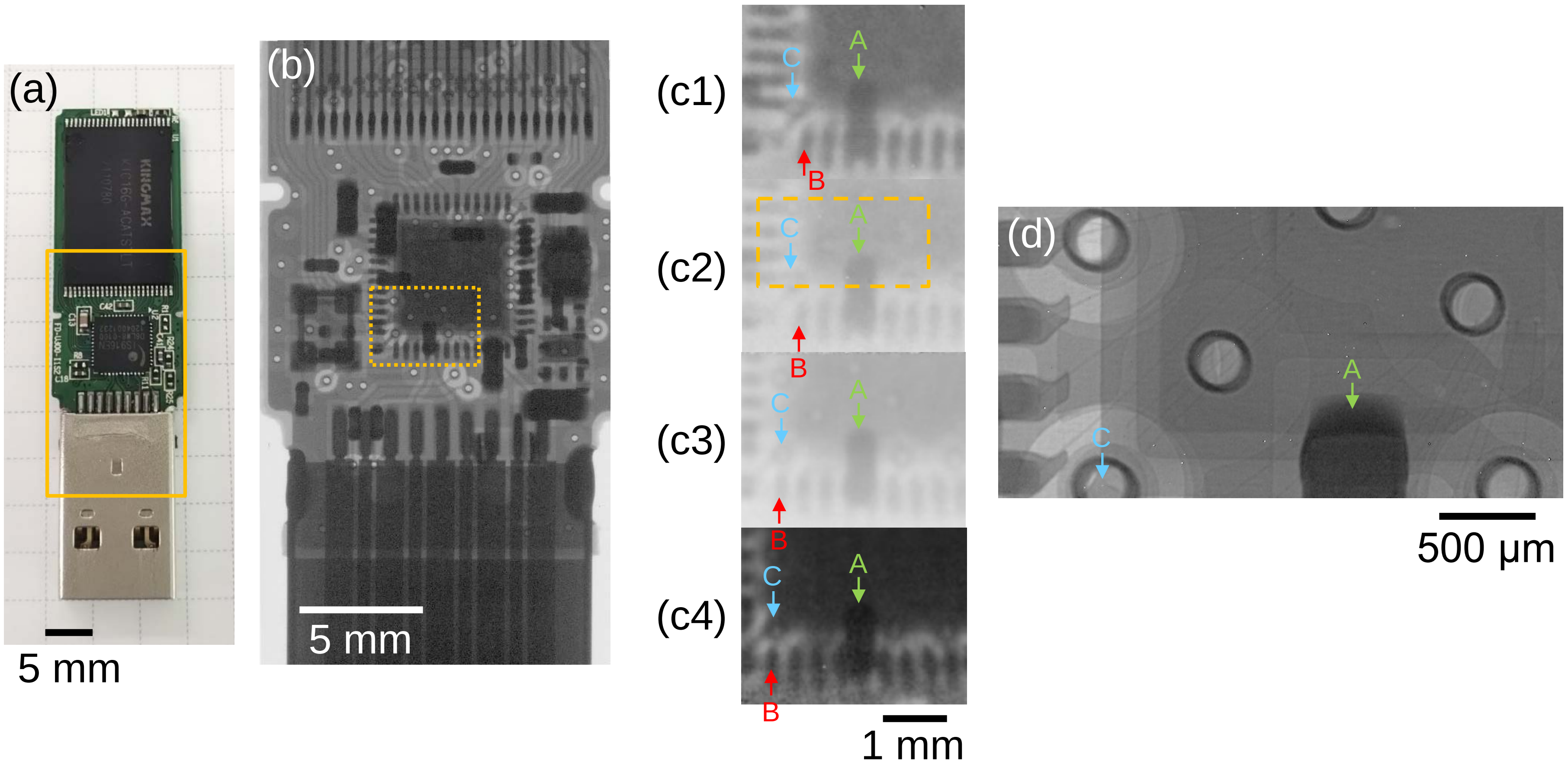

Fig. 3 W. Yashiro et al.